NUKLEONIKA 2010;55(1):91–96

ORIGINAL PAPER

Positron annihilation study of iron oxide nanoparticles in mesoporous silica MCM-41 template

Zbigniew Surowiec, Marek Wiertel, Radosław Zaleski, Mieczysław Budzyński, Jacek Goworek

Abstract. The subject of investigation were the samples obtained by impregnation of MCM-41 template with an aqueous solution prepared from $Fe(NO_3)_3 \cdot 9H_2O$. As a result of such a procedure, iron oxides deposits on MCM-41 were formed. The Mössbauer studies revealed an occurrence of Fe_3O_4 nanocrystallites in the both ferri- and superparamagnetic states. Almost 80% small particles exist in a paramagnetic state. The positron annihilation lifetime spectroscopy (PALS) spectra were measured in air or in vacuum. The long-lived *ortho*-positronium (*o*-Ps) components and their intensities are time dependent due to air molecules interaction with iron oxide nanocrystallites and silica walls surfaces. The adsorption of air on the nanocrystallites surface causes a total screening of their surface and a raise of the *o*-Ps lifetime values. Observed anti-quenching effect is a result of competition of two phenomena: practically switching off a pick-off mechanism related to interaction of *o*-Ps with magnetite nanoparticles and considerably weaker usual quenching by paramagnetic oxygen molecules.

Key words: positron annihilation • Mössbauer effect • MCM-41 porous silica • superparamagnetic nanoparticles

Z. Surowiec✉, M. Wiertel, R. Zaleski, M. Budzyński
Institute of Physics,
Maria Curie-Skłodowska University,
1 M. Curie-Skłodowskiej Sq., 20-031 Lublin, Poland,
Tel.: +48 81 537 6220, Fax: +48 81 537 6191,
E-mail: zbigniew.surowiec@umcs.lublin.pl

J. Goworek
Faculty of Chemistry,
Maria Curie-Skłodowska University,
1 M. Curie-Skłodowskiej Sq., 20-031 Lublin, Poland

Received: 29 June 2009
Accepted: 18 September 2009

Introduction

Iron oxides are important materials in technology because of their potential applications in the production of isotropic permanent magnets, high-density magnetic recording media, magnetic fluids and as a promising perspective material for spintronics [6, 10]. For such applications, a stable single-domain particle is required. This kind of materials is referred to as nanocrystalline materials in which the number of atoms in the grain boundaries is comparable to or greater than those inside the grains. However, with decreasing of the particle size the energy of their thermal motions becomes comparable with magnetic anisotropy energy and magnetic coupling between such single-domain small particles is broken and superparamagnetism phenomenon occurs. From the technological point of view, it is important to obtain optimal size of magnetic nanoparticles. The suitable method to control microscopic magnetic properties of nanocrystallites is Mössbauer spectroscopy (MS).

Nowadays, there are a lot of methods to fabricate such materials. Among the known approaches for producing nanostructures template-based methods can be distinguished [11–13, 17]. One of the popular templates used to confine conveniently magnetic compounds in low-dimensional arrays is high ordered mesoporous MCM-41 silica characterized by uniform pore diameter, large pore volume and large specific surface area [2]. Although the regular hexagonal arrangement of the cylindrical pores the in MCM-41 seems to be an almost

perfect support, the irregular distribution of silanol groups on the channel walls hinders the uniform and complete filling matrix pores. Additionally, besides the well determined cylindrical pores there exist a relatively large free volume between granules in discussed materials. A better understanding of the processes of magnetite formation and factors influencing stability of the obtained nanonstructures is necessary. PALS has been proved to be a sensitive tool for investigation of voids filling with non-magnetic material in mesoporous templates [8]. The localized *o*-Ps can undergo various interactions. It can annihilate with electrons on the pore surface by the pick-off process, in addition to the self--annihilation with a lifetime of 142 ns. Since the pick-off annihilation rate is proportional to the probability of *o*-Ps being in contact with the pore wall, the lifetime becomes shorter with decreasing pore size. Thus, *o*-Ps can be used as a porosimetric probe to evaluate the average size and size distribution of pores up to 100 nm in size. If the pores are partially or completely filled by gas/liquid molecules, pick-off annihilation with the electrons of the pore-filling molecules results in shortening of the *o*-Ps lifetime. This gives the possibility of using Ps as a microscopic probe for adsorption and pores filling [16]. In the presented work, we discuss the applicability of the PALS to control process of magnetite nanocrystallites formation in ordered silica, in particular in MCM-41.

Experimental

The mesoporous MCM-41 silica was sythesized using hexadecyltrimethylammonium bromide (C16TMAB, 96%, Aldrich) as a surfactant. The preparation procedure followed the method described in [5]. Tetraethoxysilane (TEOS, 98%, Aldrich) was used as a silica source. The as-synthesized sample was dried at 100°C for 2 h and next calcined at 550°C for 8 h. Finally, the MCM-41 sample was processed at 550°C for 5 h in an oxygen stream in order to eliminate the carbon deposit left after calcination in static conditions. In the second step the calcined samples were impregnated by inserting a 5% solution of Fe^{3+} into porous silicate for 0.5 h, drying (1 h) and calcination in air atmosphere at 300°C for 1 h. Phase analysis of impregnated sample with magnetite was carried out by means of X-ray powder diffraction (XRD) with CuK_α radiation. The presence of Fe_3O_4 was confirmed. Only a small amount of γ-Fe_2O_3 was also revealed. The average grain size 13.0(5) nm was deduced from the broadening of XRD diffraction peaks by using Sherrer's formula.

In order to characterize porosity of the MCM-41 support, the nitrogen adsorption/desorption isotherms were measured at 77 K using a volumetric adsorption analyzer ASAP 2405 (Micromeritics, Norcros, GA). The specific surface area S_{BET}, was calculated using the Brunauer--Emmett-Teller (BET) method for the desorption data in a relative pressure range p/p_0 from 0.05 to 0.25. For MCM-41 monomodal and narrow pore size distribution was obtained that is characteristic of uniform porosity of silica. The pore size distribution was calculated from the desorption isotherm by the Barrett-Joyner-Halenda procedure [1]. For the sample under study, an average pore diameter R_{BJH} = 1.5 nm, a total pore volumes V_p = 1.10 cm^3/g and a specific surface area S_{BET} = 1070 m^2/g were obtained. Magnetic properties of the nanocrystallites embedded into MCM-41 template were investigated by means of MS. Mössbauer spectra were recorded using a constant acceleration spectrometer in the wide temperature range with a $^{57}Co(Rh)$ source (1.85 GBq). The data of the Mössbauer spectra were fitted using least-squares fitting, where for magnetic component the quadrupole interaction is treated as a perturbation to the hyperfine field. The isomer shift values are given relative to α-Fe at room temperature (RT).

A study of annihilation lifetime spectra offers a non-destructive method for measuring the free volume sizes and other aspects of the environment [3] within the channels of MCM-41 mesoporous sieves. In PALS measurements the ^{22}Na positron source sealed in a Kapton envelope was placed between two layers of the powder sample, pressed together by a screwed cap inside a small copper container. The container was fixed on the top of a copper rod with a heating coil just below the sample holder. This setup was placed in a vacuum chamber allowing to obtain pressure $\sim$ 0.01 mbar. The sample temperature could be regulated from RT to over 500 K. The PALS measurements were performed at RT, if not stated otherwise. The positron lifetime spectrometer was a conventional fast-slow setup with a pulse pile-up inspection. Scintillators were BaF_2 crystals in the geometry excluding the possibility of summing effects. In the time of measuring system the start signal was produced by 1274 keV γ-ray, following the decay of ^{22}Na. The stop signal was produced by one of the annihilation photons. In porous media an essential number of *o*-Ps atoms decay into 3 gamma-quanta. Their energy spectrum is continuous, extending from 0 to 511 keV. Thus, to improve the efficiency of counting the stop energy a window in the spectrometer was widely open (80% of the energy range). At such a setting, the resolution time was 0.31 ns. The time base of the PALS spectrometer was 2 μs (8192 channels). The number of events collected per spectrum was $(2 \div 10) \times 10^6$. The lifetime spectra were analyzed using the Lifetime (LT) program [7].

Results and discussion

Mössbauer spectroscopy (MS)

In order to achieve better understanding, the magnetic finite size particles behaviour MS was applied. The obtained Mössbauer spectrum for the sample under investigation is shown in Fig. 1. The pattern measured at RT consists of two subspectra of sextet and a superimposed paramagnetic doublet. The sextets originate from Fe atoms located at two non-equivalent tetrahedral (A) and octahedral (B) sites in the magnetite. From the fitting procedure, the values of hyperfine parameters are determined. The hyperfine magnetic fields are equal to about 49.3 T and 46.0 T for tetrahedral and octahedral positions, respectively. These values are very close to those for the bulk magnetite. The presence of the doublet which could be due to some superparamagnetic relaxation is rather surprising. For such materials like bulk magnetite and maghemite which crystallize in regular structure at temperatures above T_N in the Mössbauer spectrum a monoline is observed. The existence of the

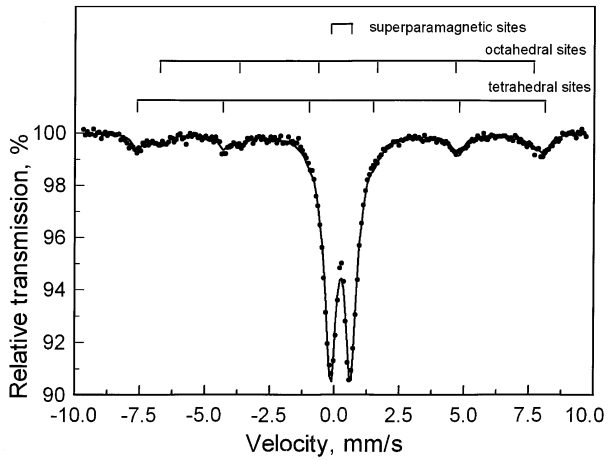

Fig. 1. The ^{57}Fe Mössbauer spectrum of Fe_3O_4/MCM-41 sample measured at RT.

superparamagnetic phenomenon for nanoparticles results from the thermal relaxation phenomenon due to the intrinsic finite-size effect. Hence one can explain the presence of superparamagnetic doublet as showing that remarkable part of Fe atoms is located in the region of the nanoparticle surface and because of the broken cubic symmetry, these atoms are exposed to non-zero electric field gradient. Additionally, the line broadening of the sextets is typical of superparamagnetic nanoparticles close to the blocking temperature, which is defined as the transition temperature from fast to slow relaxation [9]. The relative contribution of the relaxing component to the total spectrum at RT is about 80%.

With increasing temperature, the ferrimagnetic component decreases. Additionally, a monoline appears in the Mössbauer spectrum. This component results from nanoparticles in the superparamagnetic state, similarly to the doublet. However, in this case ^{57}Fe probes located in the core of nanoparticles are a source of signal. They have spherical local surroundings in which there is no electric field gradient. Appearance of the monoline at temperatures considerably below the Néel temperature for the bulk magnetite (858 K) indicates that it corresponds to a superparamagnetic phase and not to a regular paramagnetic phase.

The Mössbauer measurements unambiguously confirm the occurrence of magnetite nanocrystallites in the investigated Fe_3O_4/MCM-41 sample. However, the MS method does not give any information about localization of nanoclusters in the MCM-41 template and degree of its pores filling.

Positron annihilation lifetime spectroscopy (PALS)

Four different PAL spectra for the investigated samples are shown in Fig. 2. Significant differences in

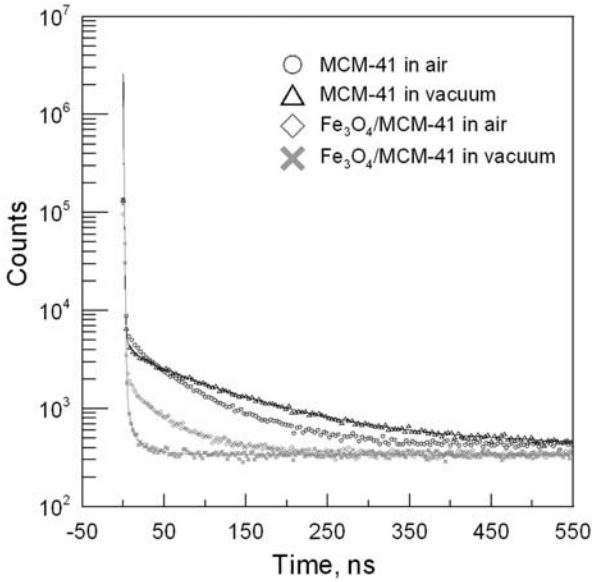

Fig. 2. Positron annihilation lifetime spectra of two MCM-41 samples impregnated with Fe_3O_4 and without impregnation measured in vacuum and in air.

the lifetimes values between the empty MCM-41 and Fe_3O_4/MCM-41 samples measured in different conditions are well visible. The spectra are rather complicated. In the fitting procedure they were assumed to consist of five exponential components: two of them are very short-lived, belonging to the decay of *para*-positronium (*p*-Ps) and the annihilation of free positrons in iron oxide particles, silica skeleton and in the Kapton envelope.

Because these lifetimes are an approximation of several undistinguishable components comparable to the time resolution of the measuring system, respective values τ_1, τ_2 are determined not too precisely: $\tau_1 \approx 0.13$ ns (*p*-Ps), $\tau_2 \approx 0.53$ ns (free e^+). In order to decrease uncertainties of the results τ_1 was fixed during fitting, what resulted in distortion of intensities of these components. However, these two components are not essential in the further considerations and inaccuracy in their determination influences *o*-Ps components only marginally [14].

Besides of the two components mentioned above, in the investigated samples of MCM-41 and Fe_3O_4/MCM-41, three long-lived *o*-Ps components were observed in the lifetime spectra. The shortest-lived of these components (τ_3) is due to *o*-Ps annihilation in the walls of nanotubes, the medium-lived one (τ_4) results from decay of *o*-Ps trapped inside of nanopores and the longest-lived among them (τ_5) is related to the annihilation of *o*-Ps trapped in free volume spaces between the grains of the material [15]. Some results of numerical fitting procedure on the asumption of five component model are listed in Table 1.

Dependence of the lifetimes and intensities of the long-lived components on air pressure for the empty

Table 1. The five-component fitting results of positron annihilation lifetime spectra of MCM-41 and Fe_3O_4/MCM-41 samples measured in vacuum ($\approx$ 0.01 mbar) and in air

Sample		τ_3 (ns)	τ_4 (ns)	τ_5 (ns)	I_3 (%)	I_4 (%)	I_5 (%)
Pure MCM-41	vacuum	6.53(42)	44.9(3.6)	128.34(87)	0.614(28)	1.99(19)	19.77(20)
	air	4.87(39)	23.3(1.3)	74.58(38)	0.664(44)	2.332(71)	14.89(16)
Fe+Fe_3O_4/MCM-41	vacuum	1.84(10)	5.07(54)	20.8(1.6)	0.81(21)	0.64(19)	0.47(19)
	air	1.84(14)	15.7(1.5)	73.8(1.5)	0.95 (20)	0.62(29)	4.38(27)

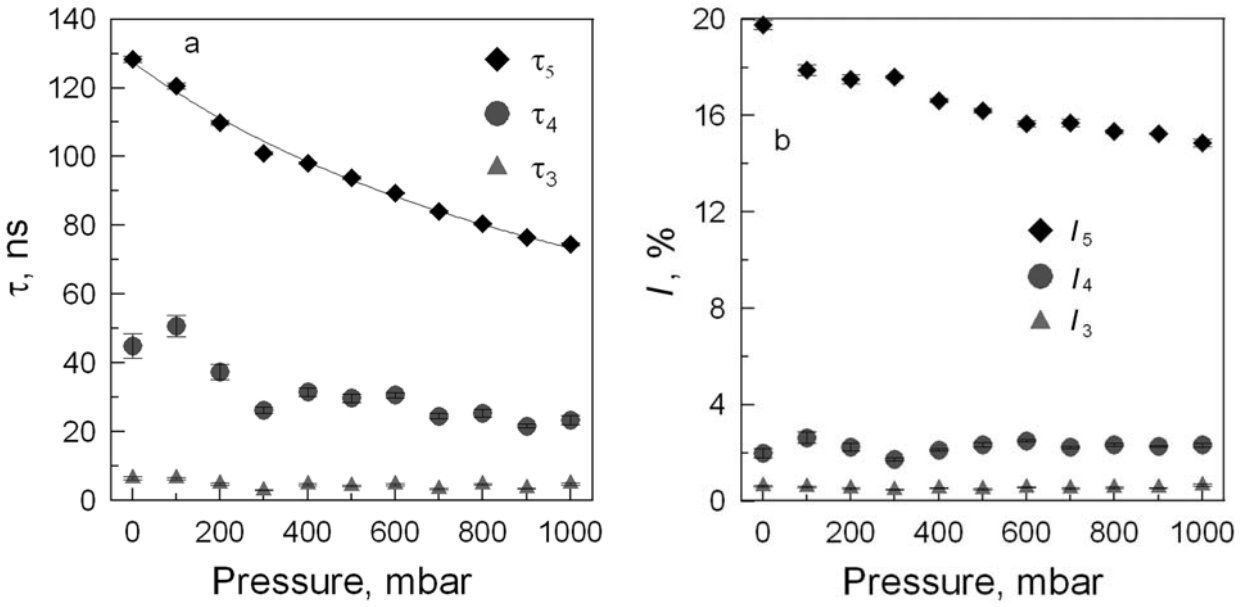

Fig. 3. The dependence of lifetimes (a) and intensities (b) of the longest components on air pressure in pure MCM-41 material measured at RT. Function described by Eq. (1) fitted to experimental τ_5 is represented by solid line.

MCM-41 silica are presented in Fig. 3. Neglecting all adsorption related processes and assuming that only constant pick-off and pressure dependent *o*-Ps air quenching by paramagnetic oxygen molecules influences τ_5, this dependence can be described by equation

$$\tau_5 = (\lambda_{p\text{-}o}^{(5)} + \lambda_q \cdot p)^{-1}, \quad (1)$$

where $\lambda_{p\text{-}o}^{(5)}$ is the pick-off probability in spaces between the grains of the material, λ_q is the air quenching rate and p is the air pressure. Values of the pick-off probability and the air quenching rate in MCM-41 were obtained by least-squares fitting of curve described by Eq. (1) to the data presented in Fig. 1.

The τ_3 remains almost constant in the whole range of pressures because either air does not penetrate small free volumes in walls of nanotubes formed from amorphous silica or air quenching rate $\lambda_q = 5.609(45)$ (μs × bar)$^{-1}$ is neglible regarding the pick-off probability in these free volumes $\lambda_{p\text{-}o}^{(3)} = 210(10)$ μs^{-1}. The τ_4 decreases remarkably, while a decrease of τ_5 is quite big. Free voids related to the last two components are of open type and quenching by an *o*-Ps to *p*-Ps conversion in interaction with paramagnetic oxygen molecules is effective ($\lambda_{p\text{-}o}^{(5)} = 7.953(27)$ μs^{-1} is comparable to λ_q). The intensity of the third and fourth components is not influenced by air pressure. The intensity I_5 decrease by about 20% when pressure increases up to ambient pressure.

Lifetime τ_5 observed in Fe_3O_4/MCM-41 composite in air is quite similar to the values observed for pure MCM-41 (Table 1). It indicates that intergranular spaces are of similar size in both samples. On the other hand, about four times smaller intensity of these components in Fe_3O_4/MCM-41 is connected to much smaller surface of the sample suggesting that a large fraction of the pores is filled with Fe_3O_4. It is also possible that Fe_3O_4 partially covers walls of these pores blocking Ps formation due to the large probability of free positron annihilation in free electron rich material. Smaller value of τ_4 in Fe_3O_4/MCM-41 seems to confirm this hypothesis.

Quite different is the relation between lifetime spectra parameters observed for Fe_3O_4/MCM-41 composite and pure MCM-41 in vacuum. A character of τ_4 and τ_5 lifetimes and appropriate intensities change is unexpected (Table 1). In the case of Fe_3O_4/MCM-41 the sample absence of air in the measuring chamber causes a considerable decrease of lifetime values in contrary to the analogous results for the empty MCM-41. Long-time evolution of the lifetimes of three long-lived components and their intensities for Fe_3O_4/MCM-41 composite is shown in Figs. 4 and 5, respectively. In details, an experimental procedure for the impregnated MCM-41 sample was as follows. The lifetime spectra were recorded in 1 h intervals at RT. The initial measurement was performed at ambient pressure and at RT. The obtained *o*-Ps lifetimes and intensities values are given in Table 1. Then, an experimental chamber was evacuated and measurements were continued during pumping. The τ_5 lifetime component abruptly jumps down to about 60 ns and then decreases. At the same time,

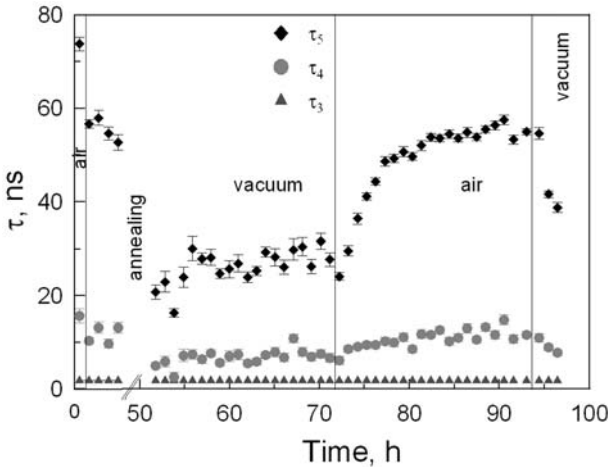

Fig. 4. Long-time evolution of the lifetimes of three long-lived components for Fe_3O_4 embedded in MCM-41. For details see the text.

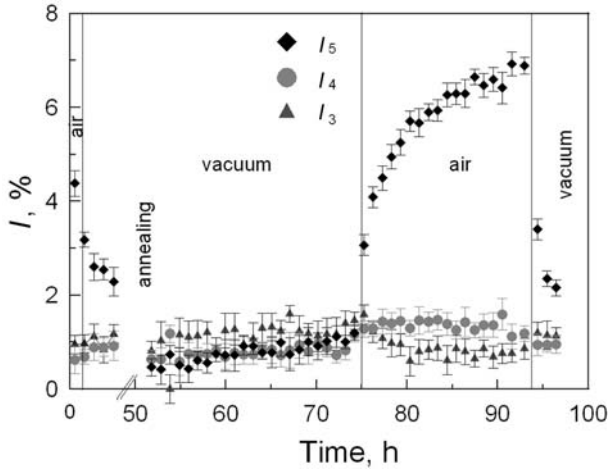

Fig. 5. Long-time evolution of the intensities of three long-lived components for Fe_3O_4 embedded in MCM-41. For details see the text.

its intensity I_5 shows similar behaviour. After 5 h, the sample was heated with stepwise increasing temperature from RT to 200°C and the spectra were collected every 4 h. Results of numerical analysis for measurements at this stage are depicted in Fig. 6. The lifetime of the longest component shortens as a result of sample degassing and achieves a value of ≈ 21 ns. The I_5 intensity drastically falls from 4.4% in air atmosphere to 0.5% after annealing. This variation is correlated with uncovering of nanocrystalline surface in this process. After self-cooling of the sample to ambient temperature, a sequence of measurements in vacuum was done and the lifetimes and intensities stayed practically constant. In the next step air was let into the chamber and the lifetime spectra were collected. The τ_5 lifetime returns to the value before annealing with a long time-constant in the order of a dozen or so hours. The corresponding intensity reveals the same tendency. It increases even above its initial value in air. The last measurements were again fulfilled in vacuum. It seems that the longest-lived component again decreases. A character of τ_4 changes is similar, but respective absolute value jumps are considerably smaller. Observed dependences confirm that channels of MCM-41 are not fully filled with Fe_3O_4 and they remain partially open.

The observed long-time evolution of the τ_5 component can be explained as follows. It is known that the adsorption of small amounts of the molecules on the pore surface increases the *o*-Ps lifetime, due to the blocking of active sites on the pore surface causing partial quenching of *o*-Ps [4]. Moreover, in water adsorption the lifetime achieves a maximum at the amount corresponding to monolayer formation, beyond which it is gradually shortened as a result of increased pick-off rate due to multilayer adsorption and pore filling. In the case of the investigated sample probably a coating of Fe_3O_4 deposits by monolayer of predominantly N_2 molecules from air takes place. The monolayer gives a film thick enough to isolate semi-metallic magnetite with a much lower electron density layer. This effect gives an opposite and predominating result to an *o*-Ps to *p*-Ps conversion in the interaction with paramagnetic air oxygen molecules.

One would suppose that hypothesis presented above should be valid also for the fourth component. Unfortunately, situation is more complicated in this case. There is an additional process consisting in the escape *o*-Ps from open hexagonal pores to interparticle spaces influencing both τ_4 and I_4. The sum of probabilities of two processes: pick-off and escape of *o*-Ps determines their values in empty MCM-41 in vacuum. Quenching by air is a third contribution to τ_4 and I_4 and quenching by Fe is fourth one. Therefore, there is a difference between the behaviour of fourth and fifth component.

Conclusions

A creation of nanocrystallites in MCM-41 template is confirmed by means of MS. The most part of them exists in superparamagnetic state at RT. The positron could create *o*-Ps and annihilate mostly in two different

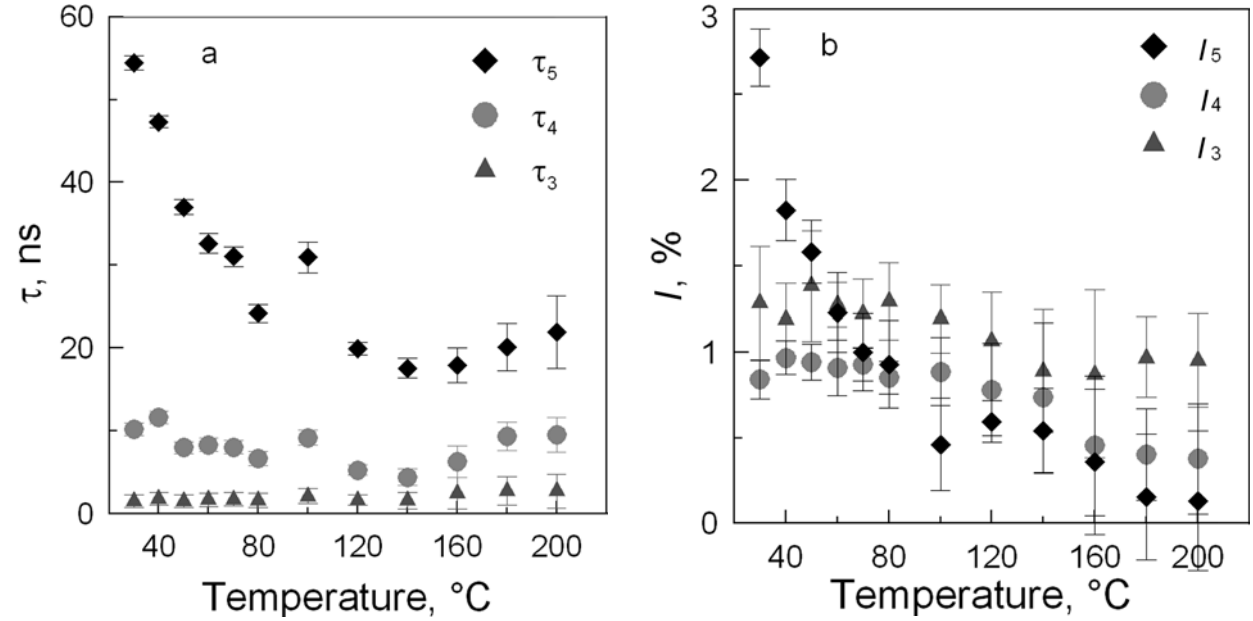

Fig. 6. The lifetimes (a) and intensities (b) of the longest components as a function of temperature for the MCM-41 impregnated with Fe_3O_4.

parts of sample volume: the free space between grains of silica and the inner space of MCM-41 nanotube capillaries with a well-defined radius. PALS supports the conclusion that the described in this paper method of impregnation MCM-41 with iron oxide enables to obtain only partial filling. The degassed Fe_3O_4 nanocrystallites surfaces interact with *o*-Ps and cause a strong quenching of *o*-Ps by pick-off process and the decreasing of Ps formation probability. For the empty MCM-41 template in annihilation processes, *o*-Ps to *p*-Ps conversion in the interaction with paramagnetic air oxygen molecules dominates.

References

1. Barrett EP, Joyner LG, Halenda PP (1951) The determination of pore volume and area distribution in porous substances. Computations from nitrogen isotherms. J Am Chem Soc 73:373–380
2. Beck JS, Vartuli JC, Roth WJ *et al*. (1992) A new family of mesoporous sieves prepared with liquid crystal templates. J Am Chem Soc 114:10834–10843
3. Boskovic S, Hill AJ, Turney TW, Gee ML, Stevens GW, O'Connor AJ (2006) Probing the microporous nature of hierarchically templated mesoporous silica via positron annihilation spectroscopy. Prog Solid State Chem 34;2/4:67–75
4. Chuang SY, Tao SJ (1971) Study of various properties of silica gel by positron annihilation. J Chem Phys 54:4902–4907
5. Grün M, Unger KK, Matsumoto A, Tsutsumi K (1997) Ordered microporous/mesoporous MCM-41 type adsorbents: novel routes in synthesis, product characterization and specification. In: McEnaney B, Mays JT, Rouquerol J, Rodriguez-Reynoso F, Sing KSW, Unger KK (eds) Characterization of porous solids IV. The Royal Society of Chemistry, London, pp 80–89
6. Gupta A, Sun JZ (1999) Spin-polarized transport and magnetoresistance in magnetic oxides. J Magn Magn Mater 200;1/3:24–43
7. Kansy J (1994) Microcomputer program for analysis of positron annihilation lifetime spectra. Nucl Instrum Methods Phys Res A 374:235–244
8. Kobayashi Y, Ito K, Oka T, Hirata K (2007) Positronium chemistry in porous materials. Radiat Phys Chem 76:224–230
9. Malini KA, Anantharaman MR, Gupta A (2004) Low temperature Mössbauer studies on magnetic nanocomposites. Bull Mater Sci 27:361–366
10. Pankhurst QA, Pollard RJ (1993) Fine-particle magnetic oxides. J Phys: Condens Matter 5:8487–8508
11. Takatani H, Fuminobu Hori F, Nakanishi M, Oshima R (2004) Positron annihilation study on Au-Pd nanoparticles prepared by sonochemical technique. Mater Sci Forum 445/446:192–194
12. Xue DS, Zhang LY, Li FS (2004) Synthesis and Mössbauer study of maghemite nanowire arrays. Hyperfine Interact 156/157:41–46
13. Yang SG, Zhu H, Yu DL, Jin ZQ, Tang SL, Du YW (2000) Preparation and magnetic property of Fe nanowire array. J Magn Magn Mater 222:97–100
14. Zaleski R (2006) Measurement and analysis of the positron annihilation lifetime spectra for mesoporous silica. Acta Phys Pol A 110:729–738
15. Zaleski R, Wawryszczuk J, Borówka A, Goworek J, Goworek T (2003) Temperature changes of the template structure in MCM-41 type materials; positron annihilation studies. Microporous Mesoporous Mater 62:47–60
16. Zhang HY, He YJ, Chen YB, Wang HY (2002) Structure and positron annihilation spectra of tin incorporated in mesoporous molecular sieves. J Appl Phys 92;12:7636–7640
17. Zhou P, Xue D, Luo H, Shi H (2002) Temperature dependence of the Mössbauer effect on prussian blue nanowires. Hyperfine Interact 142:601–606